

Jiang, L. (2023) NETWORK PHARMACOLOGY ANALYSIS OF YI-SHEN-GU-TAI-KE-LI FOR RECURRENT SPONTANEOUS ABORTION IN FEMALE FITNESS AND ATHLETIC POPULATIONS. Revista Internacional de Medicina y Ciencias de la Actividad Física y el Deporte vol. 23 (91) pp. 293-320. DOI: <https://doi.org/10.15366/rimcafd2023.91.018>

ORIGINAL

NETWORK PHARMACOLOGY ANALYSIS OF YI-SHEN-GU-TAI-KE-LI FOR RECURRENT SPONTANEOUS ABORTION IN FEMALE FITNESS AND ATHLETIC POPULATIONS

Qianqian Wan^{1, 2}, Ji Li¹, Xingxiu Zhan², Lijuan Jiang^{1*}

¹The First Clinical Medical College, Nanjing University of Traditional Chinese Medicine, Nanjing, JiangSu, 210023, China.

²Gynecology department, The First Affiliated Hospital of Yunnan University of Traditional Chinese Medicine, Kunming, Yunnan, 650021, China.

*Correspondence to: Lijuan Jiang,
Email: jianglijuan825@163.com.

UNESCO Code / UNESCO Code:

Council of Europe classification / Council of Europe classification:

Recibido 08 de abril de 2022 **Received** April 08, 2022

Aceptado 18 de junio de 2023 **Accepted** June 18, 2023

ABSTRACT

Background: Yi-Shen-Gu-Tai-Ke-Li (YSGTKL), a renowned traditional herbal formula, has demonstrated clinical efficacy in addressing recurrent spontaneous abortion (RSA). Despite its widespread utilization in China, the current body of evidence regarding the effectiveness of its herbal components remains insufficient, and the underlying mechanisms of action remain enigmatic. This study endeavors to unravel the mechanisms responsible for the therapeutic effectiveness of YSGTKL in treating RSA, particularly within the context of female fitness and athletic populations. **Methods:** YSGTKL comprises various herbal plants, selected based on the Traditional Chinese Medicine Systems Pharmacology Database and Analysis Platform (TCMSP). Specific drug targets associated with RSA were meticulously identified and corroborated using multiple reputable sources, including DrugBank, GeneCards, and Online Mendelian Inheritance in Man. The GEO database was leveraged to pinpoint differentially expressed genes (DEGs) relevant to RSA within female fitness and athletic populations. Subsequently, a comprehensive drug-compound-gene-disease network was meticulously constructed and visualized using Cytoscape software. Functional insights were gleaned through Gene Ontology (GO) annotation and Kyoto Encyclopedia of Genes and Genomes (KEGG) pathway enrichment analysis. Within this network, a subset

of hub genes was discerned through a protein-protein interaction (PPI) network analysis, specifically tailored to female fitness and athletic populations. To validate key active ingredients and core targets, molecular docking analyses were meticulously performed, taking into account the unique physiological aspects of female athletes and fitness enthusiasts. **Results:** A total of 195 active compounds were extracted from the 10 herbs constituting YSGTKL. Additionally, 8,905 common targets associated with RSA were identified from multiple comprehensive databases, with a specific focus on their relevance to female fitness and athletic populations. Subsequently, 432 DEGs were identified through the analysis of GEO datasets within this unique demographic, with 13 overlapping genes extracted from the integrated datasets. The resultant drug-compound-gene-disease network comprised 10 herbs, 123 compounds, and 13 pivotal targets, all tailored to the specific context of female fitness and athletic populations. These identified genes exhibited enrichment in several disease-related signaling pathways pertinent to this demographic. Notably, IGF2, linked to MET, IGFBP3, and ERBB3, emerged as the hub genes in the PPI network within the context of female athletes and fitness enthusiasts. Molecular docking analyses were conducted to investigate the interaction between quercetin and IGF2, considering the unique physiological characteristics of this demographic. Importantly, downregulation of IGF2 was observed in villus samples from RSA patients within female fitness and athletic populations compared to normal pregnant women. Furthermore, it was found that quercetin promoted trophoblast cell proliferation, migration, and invasion while concurrently inhibiting IGF2 expression, highlighting its potential relevance for this demographic. **Conclusion:** This study showcases the utility of network pharmacology in elucidating the effective compounds and mechanisms of action underlying the therapeutic efficacy of the YSGTKL formula in the treatment of RSA, particularly within the unique context of female fitness and athletic populations.

KEYWORDS Female Athletes, Chinese herbs, network pharmacology, recurrent spontaneous abortion, molecular docking; Fitness Enthusiasts

INTRODUCTION

Recurrent Spontaneous Abortion (RSA), the heartbreaking loss of pregnancy before the 20th week, remains a perplexing challenge in women's reproductive health. Despite advances in medical science, RSA continues to affect countless women worldwide, causing not only physical distress but also profound emotional and psychological burdens. It is a multifactorial condition influenced by genetic, hormonal, immunological, and environmental factors. Addressing RSA comprehensively requires a multifaceted approach, and traditional Chinese herbal medicine has emerged as a promising avenue for intervention (L. Li, Dou, Leung, Chung, & Wang, 2016). ("Evaluation and treatment of recurrent pregnancy loss: a committee opinion," 2012), Among the

rich tapestry of traditional Chinese herbal formulas, Yi-Shen-Gu-Tai-Ke-Li (YSGTKL) has earned a revered place. This classic herbal formula, rooted in centuries of traditional Chinese medicine (TCM) practice, has displayed considerable clinical efficacy in the management of various gynecological and obstetric conditions, including RSA (X. Chen et al., 2020; Mesdaghinia, Mohammad-Ebrahimi, Foroozanfard, & Banafshe, 2017). Its longstanding use and the encouraging outcomes it offers in China have raised hopes for more effective, holistic approaches to tackle RSA (Dimitriadis, Menkhorst, Saito, Kutteh, & Brosens, 2020). However, despite its reputation and extensive historical use, the scientific understanding of YSGTKL's pharmacological mechanisms of action remains somewhat obscure (Gangat & Tefferi, 2021). The need for empirical evidence supporting its effectiveness and a comprehensive elucidation of its mechanisms has never been more pressing, particularly within the specific demographic of female fitness and athletic populations (Chen, Chang, Kuo, & Chen, 2020; Gao et al., 2015; Lin & Qiu, 2010; Qu, Weng, & Gao, 2021).

Female athletes and fitness enthusiasts, defined by their unique physiological and hormonal profiles, represent a demographic characterized by distinct reproductive health challenges. The intense demands of their rigorous training regimens, (Czyzyk, Podfigurna, Genazzani, & Meczekalski, 2017), combined with the pressures of competition and performance goals, can profoundly affect reproductive outcomes (Carp, 2019; J. Chen et al., 2020). Given these challenges, tailored therapeutic strategies are essential. Understanding how YSGTKL operates within this specific demographic could potentially revolutionize the treatment landscape for female athletes and fitness enthusiasts grappling with RSA (Garrido-Gimenez & Alijotas-Reig, 2015; T. C. Li, Makris, Tomsu, Tuckerman, & Laird, 2002; Rai & Regan, 2006).

In this study, we endeavor to bridge the gap between the rich traditions of traditional Chinese herbal medicine and the specialized needs of female fitness and athletic populations in the context of RSA. Our approach employs the cutting-edge field of network pharmacology, a discipline that leverages advanced computational techniques to explore the multifaceted interactions between herbal compounds, molecular targets, and biological pathways. By harnessing this innovative approach, we aim to unravel the intricate web of pharmacological mechanisms underpinning YSGTKL's therapeutic effects (H. F. Li et al., 2020; Y. Q. Li et al., 2021; Nonaka et al., 2019; S. L. Yang et al., 2018; Zeng et al., 2020).

Our research objectives encompass several key facets:

1. Network Pharmacology Analysis: Through the lens of network pharmacology, we will systematically identify and analyze the active compounds contained within YSGTKL, their corresponding targets, and the intricate pathways involved in mitigating RSA.

2. Mechanistic Insights: Our study will provide a comprehensive understanding of the molecular and pharmacological mechanisms through which YSGTKL may ameliorate RSA, with a particular emphasis on the specific needs and challenges encountered by female athletes and fitness enthusiasts.

3. Safety and Efficacy Assessment: We will evaluate the safety and efficacy of YSGTKL as an adjunctive therapeutic option for RSA within the context of female fitness and athletic populations.

4. Personalized Treatment Strategies: Building upon our findings, we will propose personalized treatment strategies that incorporate YSGTKL for individuals within the female fitness and athletic community who are at risk of or currently experiencing RSA.

5. Integrating Traditional and Modern Medicine: This research aims to explore the potential synergies between traditional Chinese herbal medicine and modern healthcare practices, thereby optimizing the overall well-being and reproductive health of female athletes and fitness enthusiasts(Pan et al., 2020).

By conducting this comprehensive network pharmacology-based analysis, we seek to fill a critical knowledge gap, providing valuable insights into the potential utilization of YSGTKL as an adjunctive therapeutic approach for RSA, within the specific and dynamic demographic of female athletes and fitness enthusiasts(S. Li & Zhang, 2013). Our research not only holds the potential to contribute significantly to the reproductive health and overall well-being of these women but also exemplifies the power of interdisciplinary approaches in addressing complex healthcare challenges(Luo et al., 2020).

In the subsequent sections of this paper, we will delve into the methodology, present our findings, and engage in a thorough discussion of the implications and future prospects of this research(Bhatt, 2020; Fang, Liu, & Liu, 2020). We invite the reader to embark on this journey with us, as we explore the intersection of traditional wisdom and modern science to enhance the lives of female athletes and fitness enthusiasts facing the formidable challenge of RSA.

1. MATERIALS AND METHODS

1.1 Active compounds in Yi-Shen-Gu-Tai-Ke-Li (YSGTKL)

The Traditional Chinese Medicine Systems Pharmacology Database and Analysis Platform(TCMSP) is a data repository and analysis platform for researchers to perform comprehensive studies on Chinese herbal medicines, which contains 499 traditional Chinese herbal medicines registered in the Chinese pharmacopeia with 29384 ingredients, 3311 targets, and 837 associated diseases and comprises information of pharmaceutical chemistry, pharmacokinetics, drug likeness, drug targets, drug-target-disease network(Ru et al., 2014). Pharmacokinetic studies include the evaluation of absorption,

distribution, metabolism, and excretion (ADME) of a drug involving oral bioavailability (OB), drug-likeness (DL), intestinal epithelial permeability, blood-brain barrier, water solubility, and so on.

OB refers to the rate and extent to which administered drugs entering the circulatory system of the body it represents the percentage of the oral dose absorbed into the systemic circulation. DL refers to resemblance of a compound to a known drug. According to TCMSP, active compounds of YSGTKL were found. In our study, potential compounds of YSGTKL were screened according to the criteria of OB value $\geq 30\%$ and DL ≥ 0.18 .

1.1.1 Identification of RSA-related target genes

RSA-related target genes were obtained from DrugBank (www.drugbank.ca), GeneCards (www.genecards.org) and Online Mendelian Inheritance in Man database (OMIM, <http://omim.org>) using "recurrent spontaneous abortion" as the keyword. DrugBank database is a web-enabled database that provides information about drugs and their mechanisms, their interactions and their targets, pharmacometabolomics, pharmacotranscriptomics, pharmacoproteomics, and the status of new drug clinical trials and existing drug-repurposing trials (Valverde-Berrocoso, González-Fernández, & Acevedo-Borrega, 2022). GeneCards is a comprehensive and authoritative compendium of annotative information about human genes that were derived from over 80 digital sources and provides access to over 73,000 gene entries, encompassing the following categories: protein coding, pseudogene, RNA gene, genetic locus, cluster, and uncategorized. OMIM is also an integrative, authoritative, and timely research resource of descriptions of human genes, phenotypes, and the relationships between human genes and phenotypes (Amberger, Bocchini, Schiettecatte, Scott, & Hamosh, 2015). Then, the common genes were obtained from intersecting RSA-related target genes in the above databases.

1.1.2 Identification of differentially expressed genes (DEGs) in RSA patients

The mRNA expression data and corresponding clinical data based on endometrial pipelle biopsies of 20 women, including 10 normal pregnant women and 10 RSA women, were acquired from the Gene Expression Omnibus (GEO) datasets. The differentially expressed genes (DEGs) between RSA samples and normal endometrium samples were screened out using the Limma R package with the parameters of $|\log(\text{fold change, FC})| > 1$ and $P\text{-value} < 0.05$.

1.1.3 Identification of target genes of the active compounds in YSGTKL

Detailed information for the target genes was obtained from TCMSP database. And then names of these target genes were corrected according to

UniProt database (<http://tcmspaw.com/index.php>), and no-target compounds were found. Active compounds and their corresponding targets were identified from these databases.

1.1.4 Construction of the drug-compound-gene-disease (D-C-G-D) network

To explore the complex interactions among the drug, compounds, genes, and the disease, we constructed a comprehensive drug-compounds-genes-disease (D-C-G-D) network in this study. The overlap of target genes of active compounds and RSA-related genes was evaluated and the interaction network of the drug, compounds, targets, and the disease was constructed and visualized using Cytoscape software.

1.1.5 GO annotation and KEGG pathway enrichment analysis

GO annotation and KEGG pathway enrichment analysis were performed using clusterProfiler R package at a false discovery rate (FDR) <0.05. GO annotation is comprised of terms representing biological process (BP), molecular functions (MF), and cellular components (CC).

1.1.6 Construction of the protein-protein interaction (PPI) network

To uncover the interactive association among the targets, the protein-protein interaction network of 13 overlapping genes was constructed using STRING (<https://string-db.org/>).

1.1.7 Molecular docking of active components against potential targets

The hub targets and corresponding active compounds were screened out using Cytoscape software. The molecular docking was performed to predict the binding affinity between hub targets and corresponding active compounds. Molecular docking was employed to validate the interactions between active compound quercetin and hub target IGF2 using PyRx biological software version 0.8 (<http://pyrx.sourceforge.net>).

3D structures of IGF2 were downloaded from the Research Collaboratory for Structural Bioinformatics Protein Data Bank (RCSB PDB, <http://www.rcsb.org>), a repository of 3D biomolecular structure information, and the solvent molecules of IGF2 protein were removed using PyMOL molecular graphics system (<http://www.pymol.org>) (Seeliger & de Groot, 2010). Then, the docking study was performed using PyRx biological software version 0.8, and the automated program yielded the possible conformation with binding energy.

Comparably, the three-dimensional (3D) structure of quercetin was obtained from PubChem (<http://pubchem.ncbi.nlm.nih.gov>), which is a public repository for biological activity data of molecular and RNAi reagents (Kim et al.,

2016; Wang et al., 2012), and the information of the 3D structures of quercetin was stored at a Palm DataBase (PDB) format. The micromolecules and hydrogens were removed and then repaired the remaining structure by adding hydrogens using PyMOL molecular graphics system.

Subsequently, autoDock Vina was performed to calculate the Gasteiger charge, assigned the AutoDock 4 (AD4) type, and set all the flexible bonds of small molecular ligands to be rotatable (Trott & Olson, 2010). Then, the docking box was determined according to the original ligand coordinates. Meanwhile, the receptor protein was set to Semi-flexible docking and the molecules with the lowest binding energy in the docking conformation were selected according to the Genetic algorithm. Finally, the binding effect of the molecules was observed by matching the original ligands and intermolecular interactions and visualized using PyMOL molecular graphics system.

1.2. Experimental validation

1.2.1 Patients and samples collection

17 RSA patients and 15 elective pregnancy termination patients (normal) were recruited for this study. All patients involved in this study were aged 20-43 years and the gestational age was 5-9 weeks. The inclusion criterion of normal pregnancy patients included in this study was no history of spontaneous abortion, stillbirth, and other adverse pregnancies, no chromosomal abnormalities, no endocrine abnormalities (sex hormones, thyroid function, blood sugar levels, insulin concentration), no autoimmune diseases, no thrombosis, no reproductive malformation, tumor, abnormal uterine morphology.

This study was proved by the Ethical Committee of the First Affiliated Hospital of Yunnan University of Traditional Chinese Medicine (YNSZLL-AF-027-2021/09). And all patients included in this study knew and wrote the informed consent. The villous specimen was collected from the women with pregnancy and then stored in liquid nitrogen or 4% paraformaldehyde (PFA).

1.2.2 Immunohistochemistry (IHC) analysis

Villous tissues were fixed in 4% PFA overnight and embedded with paraffin. Then tissues were sectioned into 4- μ m. The sections were dewaxed in xylene, dehydrated in a series of gradient concentration ethanol, and antigen retrieval.

Then, the sections were incubated with primary antibody IGF2 (1:60, ab177467, Abcam, MA, USA) for 2 h and incubated with secondary antibody anti-rabbit IgG HRP-preadsorbed (1:2000, ab7090, Abcam, MA, USA) for 30 min and stained with DAB staining. The target molecules were observed and imaged under an inverted microscope.

1.2.3 Cell line and culture

The HTR-8/SVneo cell line was purchased from Zhong Qiao Xin Zhou Biotechnology Co., Ltd. (Shanghai, China), and cultured in Dulbecco's Modified Eagle Medium (DMEM, Invitrogen, Carlsbad, CA, USA) supplemented with 10% fetal bovine serum (FBS, Hyclone, South Logan, UT, USA) and 1% penicillin/streptomycin solution (Sigma-Aldrich, St. Louis, MO, USA). All cells were maintained in an incubator with 5% CO₂ at 37°C.

1.2.4 RNA extraction and quantitative reverse transcription-polymerase chain reaction (qRT-PCR)

Total RNA was extracted from villous tissues and HTR-8/SVneo cells using TRIzol reagent (Invitrogen, Carlsbad, CA, USA) according to the manufacturer's protocol. The concentration and purity were detected using Nanodrop 2000 (Invitrogen, Carlsbad, CA, USA). Reverse transcription was performed using FastKing RT Kit (With gDNase) for RT-PCR (TIANGEN, Beijing, China) according to the manufacturer's protocol. And then real-time PCR was performed using Taq Pro Universal SYBR qPCR Master Mix (Vazyme Biotech, Nanjing, China) in a LightCycler 96 system (Roche, Beijing, China). The primers in this study are the following, IGF2 (forward, 5'-AATGGGGAAGTCGATGCT-3', reverse, 5'-TCTCACTGGGGCGGTAAG-3'), GAPDH (forward, 5'-TTGCCCTCAACGACCACTTT-3', reverse, 5'-TGGTCCAGGGGTCTTACTCC-3'). Reaction conditions are as follows, 95°C, 30 s; 95°C, 15 s, 60°C, 30 s, for 40 cycles. GAPDH is a reference gene to normalize the level of IGF2. $2^{-\Delta\Delta C_t}$ was used to calculate the levels of IGF2.

1.2.5 Cell counting kit (CCK-8) assay

The HTR-8/SVneo cells in the logarithmic growth phase were collected and resuspended, then seeded in 96-well plates (Corning, NY, USA) at a density of 5000 cells each well for 24 h. Then cells were treated with increasing concentrations (0.1, 0.5, 1, 5, 10 µmol/L) of quercetin (HY-18085, MedChem Express, NJ, USA) and 1 µmol/L cyclosporine A (HY-B0579, MedChem Express, NJ, USA) for another 24 h. After that, cells were incubated with a 10 µL CCK-8 solution for 2 h. After 2 h, the absorbance was detected at 450 nm using a microplate reader (Thermo Fisher Scientific, Waltham, MA, USA). The cell viability was measured using a CCK-8 kit according to the manufacturer's protocol (Beyotime, Shanghai, China).

1.2.6 Wound healing assay

After the HTR-8/SVneo cells were stimulated with quercetin and cyclosporine A, subsequently were plated in 24-well plates (Corning, NY, USA) at a density of 1×10^5 cells per well. Cells were cultured in a complete medium until cell confluence reached 80-90%. Then changed the complete medium to

a serum-free medium to culture for 24 h. After 24 h, the wound was scratched using a 100 μ L pipette tip, the floating cells were removed. The cell migration was recorded using an electron microscope (Leica, Wetzlar, Germany) at 0 h and 24 h. The migration rate of wound closure as a percentage of the initial wound was calculated.

1.2.7 Cell invasion assay

The cell invasion was performed using the transwell chamber with an 8- μ m upper chamber (Corning, NY, USA). Briefly, after stimulating with quercetin and cyclosporine A, the HTR-8/SVneo cells were collected and resuspended in a serum-free medium for 24 h. After 24 h, 100 μ L cell suspension was added into the upper chamber, and the medium supplemented with 20% FBS (Hyclone, South Logan, UT, USA) was added into the bottom chamber. Cells were incubated in an incubator with 5% CO₂ for 24 h at 37°C. Then the cells located on the upper surface of the filter were removed using a cotton swab, and the cells located at the back of the filter were stained with 5% crystal violet (Sigma-Aldrich, St. Louis, MO, USA) for 20 min. The cell number of invasive was counted and recorded using an electron microscope (Leica, Wetzlar, Germany).

1.2.8 Western blot

Cells were lysed in RIPA lysis buffer (Beyotime, Shanghai, China) containing protease inhibitors (Sigma-Aldrich, St. Louis, MO, USA). The concentration of protein was measured using BCA Protein Assay Kit (Beyotime, Shanghai, China) according to the manufacturer's instructions. Then protein was separated by a 10% sulfate-polyacrylamide gel electrophoresis (SDS-PAGE) gel and semi-dry-transferred to a polyvinylidene fluoride membrane (PVDF, Merck Millipore, Billerica, MA, USA). The membrane was blocked with defatted milk and then incubated with special primary antibodies overnight at 4°C. After that, the membrane was washed with 1 x phosphate buffer solution (PBST) three times and then incubated with an anti-rabbit IgG HRP-link antibody (1:2000, CST7074, Cell Signaling Technology, MA, USA). The bands were visualized using Novex™ ECL Chemiluminescent Substrate Reagent Kit (Invitrogen, Carlsbad, CA, USA). The protein bands were imaged and calculated using ChemiDoc MP System (Bio-Rad, Hercules, CA, USA). The primary antibodies in this study included anti-IGF2 antibody (1:1000, ab177467, Abcam, MA, USA), and anti-GAPDH antibody (1:1000, CST2118, Cell Signaling Technology, MA, USA).

1.3. Statistical analysis

Statistical analyses in this study were performed using GraphPad Prism 8 (GraphPad Software Inc., La Jolla, CA). Data were presented as mean \pm SD. Differences between two groups were analyzed using Student's *t*-test, and differences between three groups and more than three groups were analyzed

using one-way analysis of variance (ANOVA). $P < 0.05$ was considered statistically significant.

2. RESULTS

2.1 Identification of active compounds and target genes

A total of 220 active compounds of YSGTKL were retrieved from TCMSP database fulfilling the criteria of $OB \geq 30\%$ and $DL \geq 0.18$ (Table 1), of which 10 in *Cuscutae Semen*, 20 in *Hedysarum Multijugum Maxim.*, 21 in *Codonopsis Radix*, 7 in *Atractylodes Macrocephala Koidz.*, 15 in *Poria Cocos (Schw.) Wolf.*, 2 in *Herba Taxilli*, 8 in *Dipsaci Radix*, 28 in *Eucommiae Cortex*, 16 in *Rhizoma Dioscoreae*, 92 in *licorice*. After removing duplicate compounds, 195 active compounds of YSGTKL were obtained and corresponding 296 targets were predicted using TCMSP database. RSA-related genes were predicated by searching DrugBank (PGR, ESR1, CYP17A1, NR3C1, AR, SHBG, ESR2), GeneCards, OMIM databases, and 8905 common targets were obtained by intersecting the above genes.

2.2 Identification of DEGs

We also screened the 432 DEGs (274 upregulated and 158 downregulated) in RSA compared with normal endometrial pipeline samples using the Limma R package with the threshold of $|\log(FC)| > 1$ and P -value < 0.05 (Figure 1 and 2).

2.3 Construction of a gene regulatory network

According to the predictive targets of YSGTKL, RSA-related targets, and the DEGs, 13 overlapping genes (MAOA, GABRA2, SLPI, HAS2, VCAM1, ERBB3, IGF2, IGFBP3, MET, HPSE, DPP4, PTGS2, HTR1D) were uncovered (Figure 3A). As shown in Figure 3B, a D-C-G-D regulatory network was constructed using Cytoscape, comprised of 10 herbs (*Cuscutae Semen*, *Hedysarum Multijugum Maxim.*, *Codonopsis Radix*, *Atractylodes Macrocephala Koidz.*, *Poria Cocos (Schw.) Wolf.*, *Herba Taxilli*, *Dipsaci Radix*, *Eucommiae Cortex*, *Rhizoma Dioscoreae*, *licorice.*), 123 compounds (such as quercetin, beta-sitosterol, kaempferol, etc.), and 13 targets.

2.4 Functional analysis of target genes

To illustrate the related signaling pathways involved in RSA, GO annotation analysis and KEGG pathway enrichment analysis were performed using clusterProfiler R package ($FDR < 0.05$). As shown in Figure 4A-B, multiple signaling pathways were involved in the treatment of RSA with YSGTKL, including primary amine oxidase activity, oxidoreductase activity, positive regulation of protein B signaling, and positive regulation of leukocyte cell-cells

adhesion, and proteoglycans in cancer and so on.

2.5 Construction PPI network and identification of hub genes

The significant hub genes were identified through the construction of PPI network based on the information in the STRING database. The PPI network contains 4 nodes and 14 edges. And IGF2 linked to MET, IGFBP3, and ERBB3 (Figure 5). And MAOA, GABRA2, SLPI, HAS2, VCAM1, HPSE, DPP4, PTGS2, and HTR1D have no relationship with other proteins.

2.6 Modelling quercetin-IGF2 interaction via molecular docking

Molecular docking was performed to reveal the potential binding affinity between the compound and the target (i.e. quercetin-IGF2). As shown in Figure 6A, a target binding-induced conformational change was observed. IGF2 and quercetin formed hydrogen bonds at SER 457 (B), while TYR 508 (B) connects to IGF2 via π - π bounds and LYS 552 (B) attaches to IGF2 via π -cation bounds (Figure 6B). The molecular docking confirmed the binding interactions between quercetin and IGF2.

2.7 Upregulated IGF2 in the villous specimen from RSA patients

The bioinformatics analysis has demonstrated that IGF2 was an important therapeutic target in the treatment of RSA patients. Hence, we carried out an investigation by comparing the expression of IGF2 in RSA patients with that of normal pregnant women. As shown in Figure 7A-B, the villus samples of RSA patients exhibited increased IGF2 levels and the qRT-PCR results indicated that IGF2 was strongly upregulated in villus samples of RSA patients compared with normal pregnant women (Figure 7C).

2.8 Promoting effects of quercetin on cell proliferation

We investigated the effects of quercetin on the phenotype of trophoblasts using the HTR-8/SVneo cell line. Cyclosporine A-treated HTR-8/SVneo cells served as a positive control in this study. The CCK-8 results indicated that quercetin promoted cell proliferation in a dose- and time-dependent manner (Figure 8A-C). Besides, the colony formation also revealed that quercetin enhanced the cell viability in a dose-dependent manner (Figure 8D-E). These findings suggested the positive effects of quercetin on trophoblast growth (Ramis, 2017).

2.9 Facilitating effects of quercetin on cell migration and invasion

We further investigated the effects of quercetin on the migration and invasion of HTR-8/SVneo cells. The results indicated that increasing concentration of quercetin promoted the migration and invasion abilities of HTR-8/SVneo cells (Figure 9A-D). These results indicated that quercetin could

increase the migration and invasion abilities of trophoblasts.

2.10 Inhibitory effects of quercetin on IGF2 expression in HTR-8/SVneo cells

Bioinformatic analysis proved that quercetin in YSGTKL targeted IGF2 to alleviate symptoms of RSA. Therefore, we explored the expression of IGF2 in HTR-8/SVneo cells before and after stimulating the quercetin. The results indicated that increasing the concentration of quercetin significantly inhibited mRNA and protein levels of IGF2 in HTR-8/SVneo cells compared with the control group (Figure 10A-C). These findings revealed that IGF2 was the target of quercetin.

3. DISCUSSION

Though TCM is the greatest treasure in human medicine and has given birth to holistic approaches in the diagnosis and treatment of diseases which include traditional herbal prescriptions that predated modern science. These traditional herbal prescriptions are developed based on thousands of years of phenotype-based and personalized human clinical trials (F. S. Li & Weng, 2017), which lack scientific and clinical evidence support for safety, efficacy and potential mechanisms hindering their clinical applications. Therefore, it's necessary to explore and study the bioactive compounds, main targets, regulatory mechanisms, and pharmacological activities of TCM using modern scientific and reliable methods.

In the present study, based on the network pharmacology, we identified 195 compounds from the 10 herbs of YSGTKL and screened out 13 targets (MAOA, GABRA2, SLPI, HAS2, VCAM1, ERBB3, IGF2, IGFBP3, MET, HPSE, DPP4, PTGS2, HTR1D) from common genes among GeneCards, OMIM, Drugbank, GEO database. Then, 10 drugs, 123 active compounds (such as glycitein, gancaonin H, isolicoflavonol, licoisoflavanone, glepidotin B, glyzaglabrin, and quercetin), and 13 hub targets were used to establish the disease-drug-compound-target network. The GO and KEGG pathways enrichment were further performed, and the GO annotation enrichment analysis indicated that these targets are associated with disease signaling pathways, including primary amine oxidase activity, oxidoreductase activity, positive regulation of protein B signaling, and positive regulation of leukocyte cell-cell adhesion. However, the KEGG pathway enrichment analysis revealed that these targets enriched proteoglycans in cancer. In addition, we identified the hub targets by constructing a PPI network, and the IGF2 was identified as the hub target in the network with the highest degree. The molecular docking was performed to mimic the connection between IGF2 and quercetin. IGF2 has been identified as a genetic susceptibility gene in RSA (Ardeshir, Keshavarz, Asadian, Omidmokhtarkhanloo, & Yavarian, 2020; Perez et al., 2012), it is the

major fetal growth factor that regulates fetoplacental growth, a potent mitogen to promote autocrine effects on preimplantation development, and a regulator in diffusional exchange of the placenta (Ostojić, Pereza, Volk, Kapović, & Peterlin, 2008). Here, we found abnormal expression of IGF2 in RSA, and mainly severed as a target of quercetin. And we demonstrated that IGF2 expression was significantly upregulated in villus samples of RSA patients compared with normal pregnant women.

Quercetin is a natural polyphenol that abundantly exists in plants and its biological functions in diseases has been demonstrated in numerous studies as antioxidant, anti-inflammatory, immunoregulation, and anticancer. For example, quercetin ameliorates nonalcoholic fatty liver in db/db mice by inhibiting inflammation, oxidative stress, and lipid metabolism (H. Yang et al., 2019). Quercetin exerts anticancer effects in prostate cancer by the modulation of ROS production, and in breast cancer by inducing apoptosis and necroptosis. Hyperoside, also known as quercetin 3-D-galactoside, has been found that can attenuate pregnancy loss in a RSA rat model by inducing autophagy and inhibiting inflammation. In the present study, we identified quercetin from the *Cuscutae Semen*, *edysarum Multijugum Maxim.*, *Herba Taxilli*, *Eucommiae Cortex*, and *licorice*. These results indicated that quercetin might play a crucial role in the treatment of RSA. Moreover, we validated the interaction between IGF2 and quercetin by performing molecular docking and the results indicated that IGF2 was connected to quercetin by hydrogen bonds, π - π bounds, and π -cation bounds. Based on cellular experiments, we demonstrated that quercetin could significantly promote cell proliferation, migration, and invasion, and reduce the IGF2 expression at transcriptomic and post-transcriptomic levels.

4. CONCLUSION

In conclusion, this study employed network pharmacology to investigate the mechanisms underlying the therapeutic effectiveness of the traditional Chinese herbal formula Yi-Shen-Gu-Tai-Ke-Li (YSGTKL) in the context of recurrent spontaneous abortion (RSA), with a specific focus on female fitness and athletic populations. The key findings of this research shed light on the potential application of YSGTKL in addressing RSA within this unique demographic.

Through a comprehensive analysis, we identified the active compounds and their targets within YSGTKL, confirming their relevance to RSA. Additionally, we explored the differentially expressed genes (DEGs) associated with RSA in female athletes and fitness enthusiasts, shedding light on the intricate molecular pathways involved. The construction of a drug-compound-gene-disease network revealed the complex interplay between the herbal components, their molecular targets, and the biological processes implicated in RSA. This network analysis provided a comprehensive view of the

pharmacological mechanisms underlying YSGTKL's therapeutic effects, specifically tailored to female fitness and athletic populations.

Notably, the identification of hub genes, including GF2 linked to MET, IGFBP3, and ERBB3, highlighted potential key players in the treatment of RSA within this demographic. Moreover, molecular docking analysis, considering the unique physiological characteristics of female athletes and fitness enthusiasts, provided valuable insights into the interactions between quercetin and IGF2, reinforcing the relevance of YSGTKL in promoting trophoblast cell proliferation and inhibiting IGF2 expression. In essence, this study exemplifies the power of network pharmacology in elucidating the mechanisms of action of traditional herbal formulas like YSGTKL in addressing RSA, with a specific focus on the distinct needs and challenges faced by female fitness and athletic populations. These findings open up new avenues for holistic and personalized treatment strategies that may benefit the reproductive health and overall well-being of female athletes and fitness enthusiasts dealing with recurrent spontaneous abortion. Further research and clinical studies are warranted to validate the therapeutic potential of YSGTKL within this unique demographic and to advance the integration of traditional Chinese medicine into modern healthcare practices for female athletes and fitness enthusiasts.

Data availability statement

The raw data supporting the conclusion of this article are included in the supplementary files (<https://github.com/jianqlijuan825/Supplementary-files-.git>).

Author contribution

Conceptualization: LiJuan Jiang. Data curation: Qianqian Wan. Formal analysis: Ji Li and Xingxiu Zhan. Investigation: Qianqian Wan. Methodology: Ji Li and Xingxiu Zhan. Project administration: LiJuan Jiang. Writing the original draft: Qianqian Wan. Reviewing and editing the article: Lijuan Jiang.

Funding

This study was supported by the National Natural Science Foundation of China (82060882).

ACKNOWLEDGMENTS

The authors sincerely acknowledge the support of the National Natural Science Foundation of China (82060882).

REFERENCES

Amberger, J. S., Bocchini, C. A., Schiettecatte, F., Scott, A. F., & Hamosh, A. (2015). OMIM.org: Online Mendelian Inheritance in Man (OMIM®), an

- online catalog of human genes and genetic disorders. *Nucleic Acids Res*, 43(Database issue), D789-798. doi:10.1093/nar/gku1205
- Ardeshir, F., Keshavarz, L., Asadian, F., Omidmokhtarkhanloo, G., & Yavarian, M. (2020). Role of the 820 A/G variant in the IGF-2 gene and recurrent spontaneous abortion in southern Iran: A cross-sectional study. *Int J Reprod Biomed*, 18(9), 747-754. doi:10.18502/ijrm.v13i9.7669
- Bhatt, S. M. (2020). A Critical Review On Nano-Food Packaging and Its Applications. *Journal of Commercial Biotechnology*, 25(3), 3-17. doi:<https://doi.org/10.5912/jcb882>
- Carp, H. (2019). Immunotherapy for recurrent pregnancy loss. *Best Pract Res Clin Obstet Gynaecol*, 60, 77-86. doi:10.1016/j.bpobgyn.2019.07.005
- Chen, J., Liu, B., Zhang, Y., Ao, L., Li, Z., Qu, B., . . . Yang, J. (2020). Effect of immunotherapy on patients with unexplained recurrent spontaneous abortion. *Ann Palliat Med*, 9(5), 2545-2550. doi:10.21037/apm-19-440b
- Chen, S. L., Chang, S. M., Kuo, P. L., & Chen, C. H. (2020). Stress, anxiety and depression perceived by couples with recurrent miscarriage. *Int J Nurs Pract*, 26(2), e12796. doi:10.1111/ijn.12796
- Chen, X., Diao, L., Lian, R., Qi, L., Yu, S., Liu, S., . . . Zeng, Y. (2020). Potential impact of maternal vitamin D status on peripheral blood and endometrium cellular immunity in women with recurrent implantation failure. *Am J Reprod Immunol*, 84(1), e13243. doi:10.1111/aji.13243
- Czyzyk, A., Podfigurna, A., Genazzani, A. R., & Meczekalski, B. (2017). The role of progesterone therapy in early pregnancy: from physiological role to therapeutic utility. *Gynecol Endocrinol*, 33(6), 421-424. doi:10.1080/09513590.2017.1291615
- Dimitriadis, E., Menkhorst, E., Saito, S., Kutteh, W. H., & Brosens, J. J. (2020). Recurrent pregnancy loss. *Nat Rev Dis Primers*, 6(1), 98. doi:10.1038/s41572-020-00228-z
- Evaluation and treatment of recurrent pregnancy loss: a committee opinion. (2012). *Fertil Steril*, 98(5), 1103-1111. doi:10.1016/j.fertnstert.2012.06.048
- Fang, T., Liu, L., & Liu, W. (2020). Network pharmacology-based strategy for predicting therapy targets of *Tripterygium wilfordii* on acute myeloid leukemia. *Medicine (Baltimore)*, 99(50), e23546. doi:10.1097/md.00000000000023546
- Gangat, N., & Tefferi, A. (2021). Myeloproliferative neoplasms and pregnancy: Overview and practice recommendations. *Am J Hematol*, 96(3), 354-366. doi:10.1002/ajh.26067
- Gao, J., Deng, G., Hu, Y., Huang, Y., Lu, L., Huang, D., . . . Luo, S. (2015). Quality of reporting on randomized controlled trials on recurrent spontaneous abortion in China. *Trials*, 16, 172. doi:10.1186/s13063-015-0665-6
- Garrido-Gimenez, C., & Alijotas-Reig, J. (2015). Recurrent miscarriage: causes, evaluation and management. *Postgrad Med J*, 91(1073), 151-162.

doi:10.1136/postgradmedj-2014-132672

- Kim, S., Thiessen, P. A., Bolton, E. E., Chen, J., Fu, G., Gindulyte, A., . . . Bryant, S. H. (2016). PubChem Substance and Compound databases. *Nucleic Acids Res*, 44(D1), D1202-1213. doi:10.1093/nar/gkv951
- Li, F. S., & Weng, J. K. (2017). Demystifying traditional herbal medicine with modern approach. *Nat Plants*, 3, 17109. doi:10.1038/nplants.2017.109
- Li, H. F., Shen, Q. H., Li, X. Q., Feng, Z. F., Chen, W. M., Qian, J. H., . . . Yang, Y. (2020). The Efficacy of Traditional Chinese Medicine Shoutai Pill Combined with Western Medicine in the First Trimester of Pregnancy in Women with Unexplained Recurrent Spontaneous Abortion: A Systematic Review and Meta-Analysis. *Biomed Res Int*, 2020, 7495161. doi:10.1155/2020/7495161
- Li, L., Dou, L., Leung, P. C., Chung, T. K., & Wang, C. C. (2016). Chinese herbal medicines for unexplained recurrent miscarriage. *Cochrane Database Syst Rev*, 2016(1), Cd010568. doi:10.1002/14651858.CD010568.pub2
- Li, S., & Zhang, B. (2013). Traditional Chinese medicine network pharmacology: theory, methodology and application. *Chin J Nat Med*, 11(2), 110-120. doi:10.1016/s1875-5364(13)60037-0
- Li, T. C., Makris, M., Tomsu, M., Tuckerman, E., & Laird, S. (2002). Recurrent miscarriage: aetiology, management and prognosis. *Hum Reprod Update*, 8(5), 463-481. doi:10.1093/humupd/8.5.463
- Li, Y. Q., Li, W. L., Yu, X. H., Wu, H., Wang, Y. Z., Jin, Y., . . . Song, X. G. (2021). Mechanisms of Traditional Chinese Medicine Bushenantai granules in promoting angiogenesis at the maternal-fetal interface of recurrent spontaneous abortion mice. *J Tradit Chin Med*, 41(4), 556-563. doi:10.19852/j.cnki.jtcm.20210319.001
- Lin, Q. D., & Qiu, L. H. (2010). Pathogenesis, diagnosis, and treatment of recurrent spontaneous abortion with immune type. *Front Med China*, 4(3), 275-279. doi:10.1007/s11684-010-0101-y
- Luo, T. T., Lu, Y., Yan, S. K., Xiao, X., Rong, X. L., & Guo, J. (2020). Network Pharmacology in Research of Chinese Medicine Formula: Methodology, Application and Prospective. *Chin J Integr Med*, 26(1), 72-80. doi:10.1007/s11655-019-3064-0
- Mesdaghinia, E., Mohammad-Ebrahimi, B., Foroozanfard, F., & Banafshe, H. R. (2017). The effect of vitamin E and aspirin on the uterine artery blood flow in women with recurrent abortion: A single-blind randomized controlled trial. *Int J Reprod Biomed*, 15(10), 635-640.
- Nonaka, T., Takahashi, M., Nonaka, C., Haino, K., Yamaguchi, M., Enomoto, T., & Takakuwa, K. (2019). Treatment for patients with recurrent fetal losses positive for anti-cardiolipin beta2 glycoprotein I antibody using Sairei-to (Chai-ling-tang) and low-dose aspirin. *J Obstet Gynaecol Res*, 45(3), 549-555. doi:10.1111/jog.13871
- Ostojić, S., Perez, N., Volk, M., Kapović, M., & Peterlin, B. (2008). Genetic predisposition to idiopathic recurrent spontaneous abortion: contribution

- of genetic variations in IGF-2 and H19 imprinted genes. *Am J Reprod Immunol*, 60(2), 111-117. doi:10.1111/j.1600-0897.2008.00601.x
- Pan, L., Li, Z., Wang, Y., Zhang, B., Liu, G., & Liu, J. (2020). Network pharmacology and metabolomics study on the intervention of traditional Chinese medicine Huanglian Decoction in rats with type 2 diabetes mellitus. *J Ethnopharmacol*, 258, 112842. doi:10.1016/j.jep.2020.112842
- Pereza, N., Ostojić, S., Volk, M., Maver, A., Kapović, M., & Peterlin, B. (2012). The insulin-like growth factor 2 receptor gene Gly1619Arg polymorphism and idiopathic recurrent spontaneous abortion. *J Matern Fetal Neonatal Med*, 25(4), 429-431. doi:10.3109/14767058.2011.581713
- Qu, J., Weng, X. L., & Gao, L. L. (2021). Anxiety, depression and social support across pregnancy in women with a history of recurrent miscarriage: A prospective study. *Int J Nurs Pract*, 27(5), e12997. doi:10.1111/ijn.12997
- Rai, R., & Regan, L. (2006). Recurrent miscarriage. *Lancet*, 368(9535), 601-611. doi:10.1016/s0140-6736(06)69204-0
- Ramis, I. B. (2017). Molecular methods for detection of Helicobacter pylori infection: could they be the gold standard? In (Vol. 53, pp. 4-4): SciELO Brasil.
- Ru, J., Li, P., Wang, J., Zhou, W., Li, B., Huang, C., . . . Yang, L. (2014). TCMSP: a database of systems pharmacology for drug discovery from herbal medicines. *J Cheminform*, 6, 13. doi:10.1186/1758-2946-6-13
- Seeliger, D., & de Groot, B. L. (2010). Ligand docking and binding site analysis with PyMOL and Autodock/Vina. *J Comput Aided Mol Des*, 24(5), 417-422. doi:10.1007/s10822-010-9352-6
- Trott, O., & Olson, A. J. (2010). AutoDock Vina: improving the speed and accuracy of docking with a new scoring function, efficient optimization, and multithreading. *J Comput Chem*, 31(2), 455-461. doi:10.1002/jcc.21334
- Valverde-Berrocoso, J., González-Fernández, A., & Acevedo-Borrega, J. (2022). Disinformation and multiliteracy: A systematic review of the literature. *Comunicar*, 30(70), 97-110.
- Wang, Y., Xiao, J., Suzek, T. O., Zhang, J., Wang, J., Zhou, Z., . . . Bryant, S. H. (2012). PubChem's BioAssay Database. *Nucleic Acids Res*, 40(Database issue), D400-412. doi:10.1093/nar/gkr1132
- Yang, H., Yang, T., Heng, C., Zhou, Y., Jiang, Z., Qian, X., . . . Lu, Q. (2019). Quercetin improves nonalcoholic fatty liver by ameliorating inflammation, oxidative stress, and lipid metabolism in db/db mice. *Phytother Res*, 33(12), 3140-3152. doi:10.1002/ptr.6486
- Yang, S. L., Niu, T. T., Li, X. L., Li, D. J., Li, M. Q., & Wang, H. Y. (2018). Bu-Shen-Yi-Qi formula impairs cytotoxicity of NK cells by up-regulating IDO expression in trophoblasts. *Gynecol Endocrinol*, 34(8), 675-679. doi:10.1080/09513590.2018.1425988
- Zeng, L., Yang, K., Liu, L., Zhang, T., Liu, H., Tan, Z., & Lei, L. (2020).

Systematic biological and proteomics strategies to explore the regulation mechanism of Shoutai Wan on recurrent spontaneous Abortion's biological network. *J Ethnopharmacol*, 263, 113156. doi:10.1016/j.jep.2020.113156

Figure legends

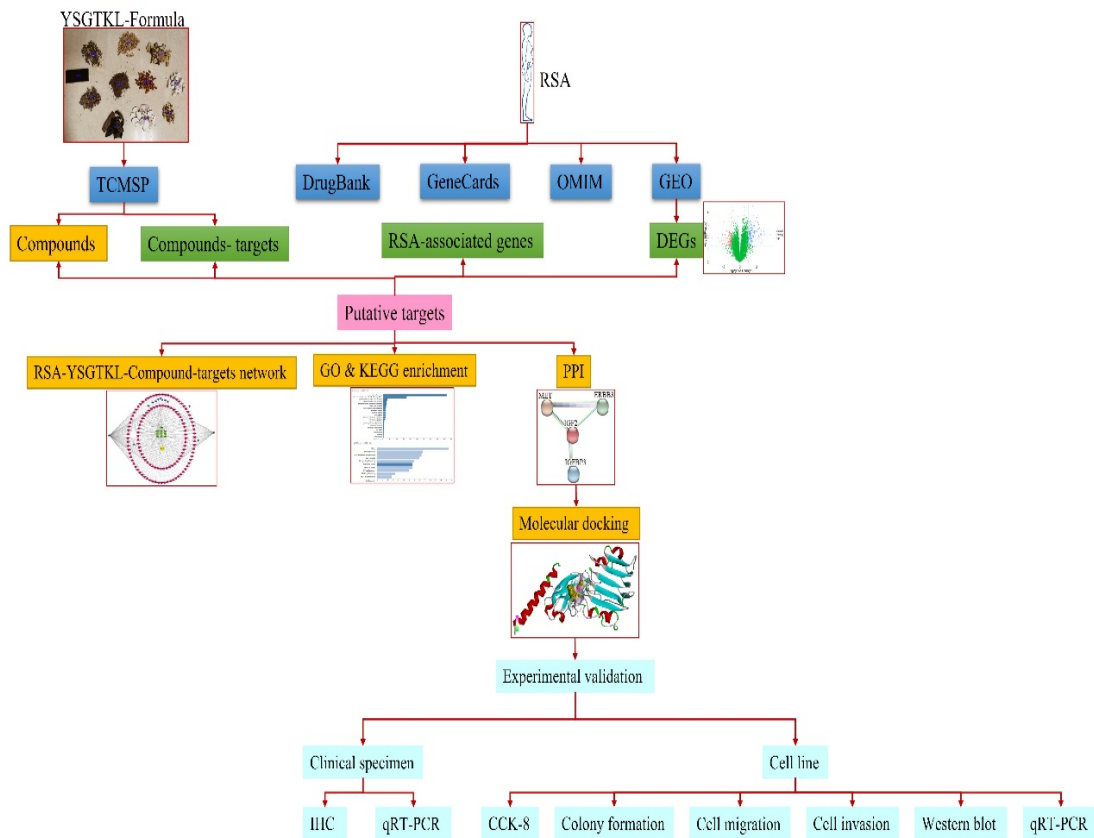


Figure 1: Flowchart of the network pharmacology for identifying the therapeutic mechanisms of action of Yi-Shen-Gu-Tai-Ke-Li (YSGTKL) on recurrent spontaneous abortion (RSA).

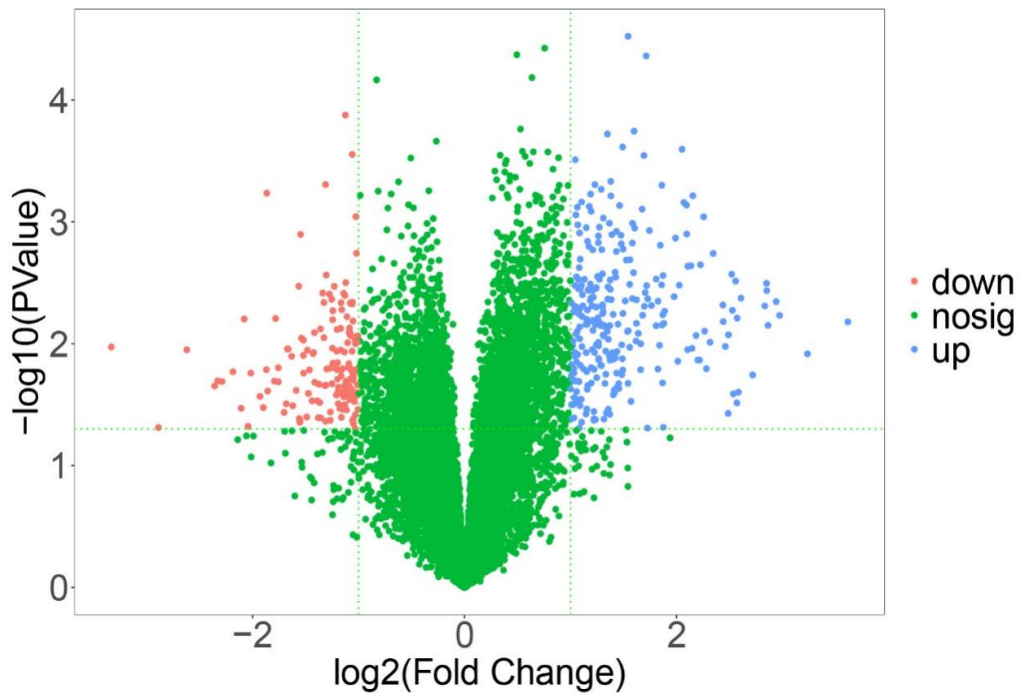


Figure 2: Volcano plot described the differentially expressed genes (DEGs) in RSA. Blue dots indicated upregulated DEGs, and red dots indicated downregulated DEGs.

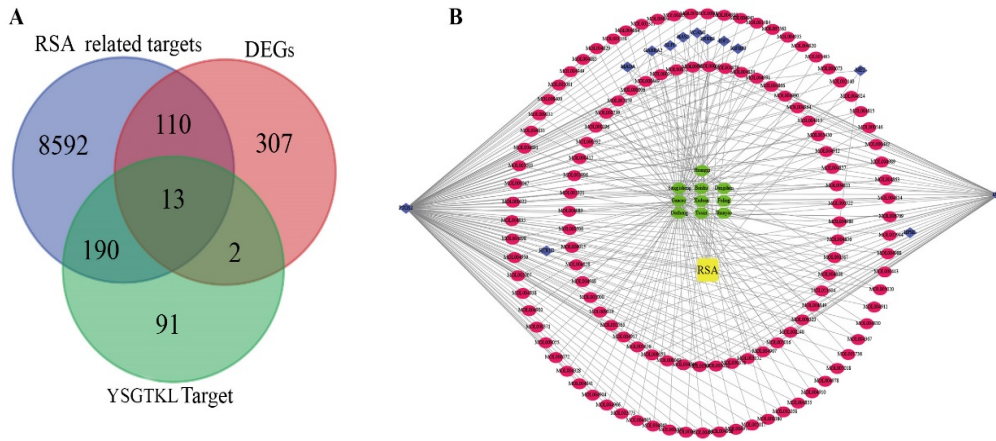


Figure 3: Screening the targets of compounds of YSGTKL formula and constructing the drug-compounds-genes-disease network.

(A) Venn diagram indicated the common genes by intersecting YSGTKL-targets, RSA-related targets, and DEGs among DrugBank, GeneCards, OMIM, and GEO databases.

(B) The potential drug-compounds-genes-disease network of YSGTKL in the treatment of RSA.

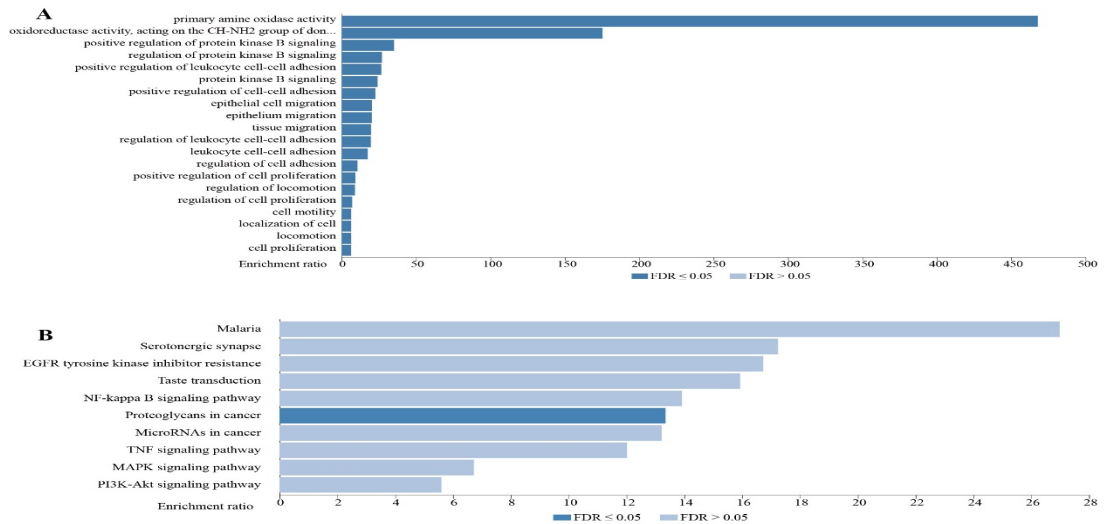


Figure 4: GO annotation (A) and KEGG pathways (B) enrichment analysis.

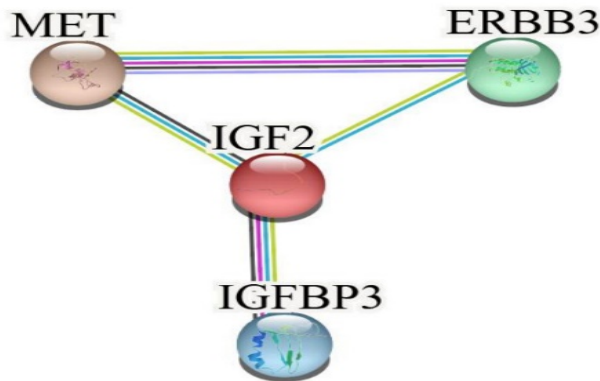


Figure 5: Protein-protein interaction (PPI) network of 13 targets of compounds.

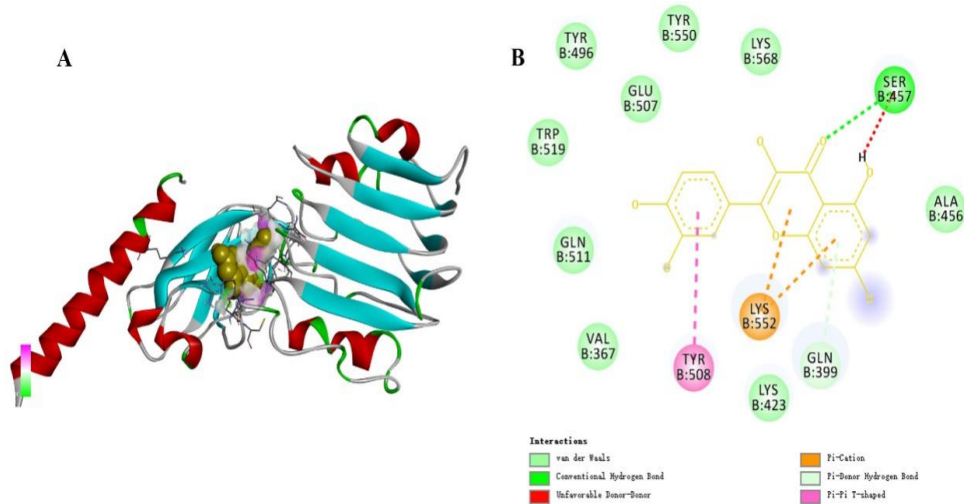


Figure 6: Active components-targets docking.

(A) 3-D binding model of IGF2 and quercetin. The ball-and-stick model represented molecules.

(B) 2-D binding model of IGF2 and quercetin.

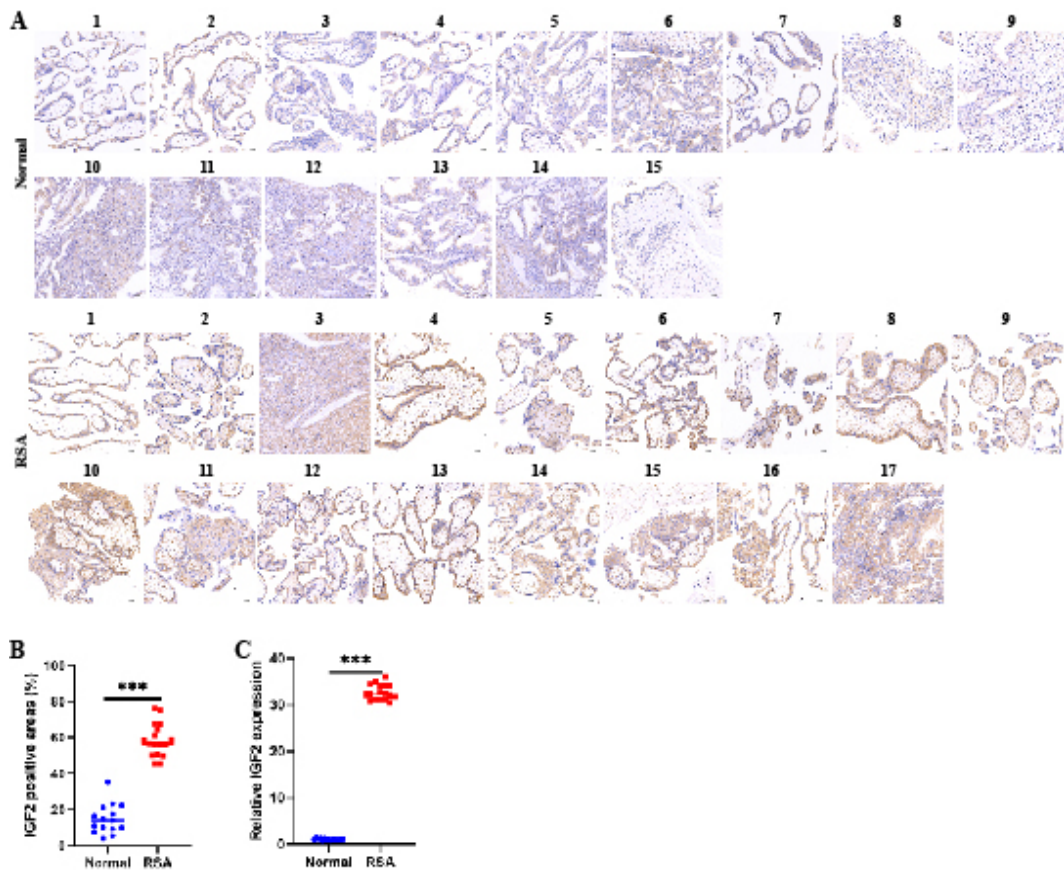


Figure 7 Upregulated IGF2 in the villous specimen of human RSA patients.

(A)-(B) IHC analysis of the IGF2 expression in villous samples of RSA patients and normal pregnant women (Scale bar = 100 μ m).

(C) qRT-PCR analysis of the expression of IGF2 between villous samples of RSA patients and normal pregnant women.

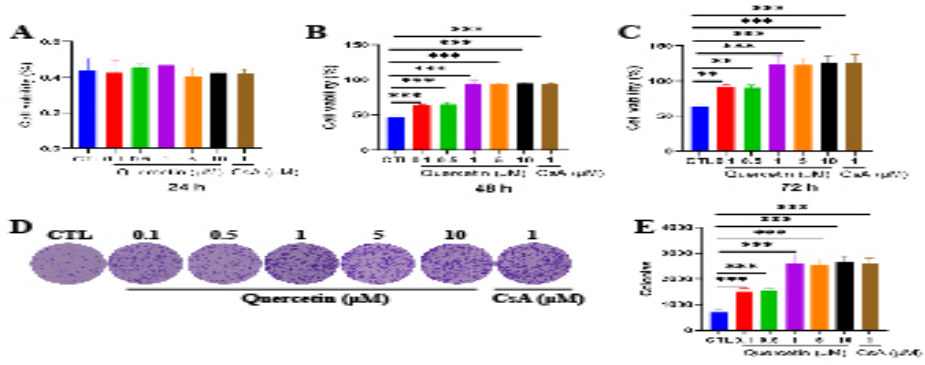


Figure 8 Quercetin promotes cell proliferation.

(A)-(C) CCK-8 assay was performed to detect the cell viability at 24 h, 48 h, and 72 h by stimulating with increasing concentration (0.1, 0.5, 1, 5, 10 $\mu\text{mol/L}$) of quercetin and 1 $\mu\text{mol/L}$ cyclosporine A. (D)-(E) Colony formation assay was used to investigate the cell colony ability by stimulating with increasing concentration (0.1, 0.5, 1, 5, 10 $\mu\text{mol/L}$) of quercetin and 1 $\mu\text{mol/L}$ cyclosporine A.

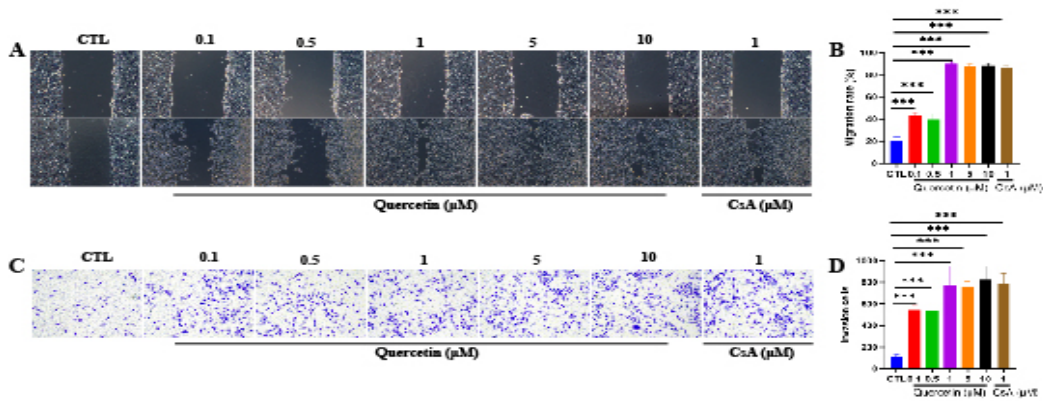


Figure 9 Quercetin enhances cell migration and invasion.

(A)-(B) Wound healing assay was used to detect the migration ability by stimulating with increasing concentration (0.1, 0.5, 1, 5, 10 $\mu\text{mol/L}$) of quercetin and 1 $\mu\text{mol/L}$ cyclosporine A (Scale bar = 100 μm). (C)-(D) Transwell assay was performed to examine the invasion ability by stimulating with increasing concentration (0.1, 0.5, 1, 5, 10 $\mu\text{mol/L}$) of quercetin and 1 $\mu\text{mol/L}$ cyclosporine A (Scale bar = 100 μm).

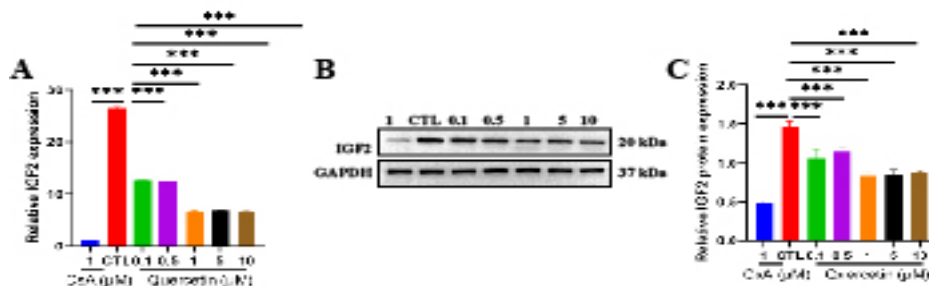


Figure 10 Quercetin inhibits IGF2 expression in HTR-8/SVneo cells.

(A) RT-PCR analysis of the expression of IGF2 in HTR-8/SVneo cells by stimulating with increasing concentration (0.1, 0.5, 1, 5, 10 $\mu\text{mol/L}$) of quercetin and 1 $\mu\text{mol/L}$ cyclosporine A. (B)-(C) Western blot analysis of the protein levels of IGF2 in HTR-8/SVneo cells by stimulating with increasing concentration (0.1, 0.5, 1, 5, 10 $\mu\text{mol/L}$) of quercetin and 1 $\mu\text{mol/L}$ cyclosporine A.

Table 1: Compounds in YSGTKL obtained from TCMSp database (OB≥30%, and DL≥0.18).

MOL ID	MOLECULE ID	MOLECULE NAME	OB	DL
MOL001558	Tusizi	Sesamin	56.54706	0.82722
MOL000184	Tusizi	NSC63551	39.25365	0.7594
MOL000354	Tusizi	Isorhamnetin	49.60438	0.306
MOL000358	Tusizi	Beta-sitosterol	36.91391	0.75123
MOL000422	Tusizi	Kaempferol	41.88225	0.24066
MOL005043	Tusizi	Campest-5-en-3beta-ol	37.57682	0.71481
MOL005440	Tusizi	Isofucosterol	43.7764	0.7576
MOL005944	Tusizi	Matrine	63.77493	0.24931
MOL006649	Tusizi	Sophranol	55.41662	0.28192
MOL000953	Tusizi	CLR	37.8739	0.67677
MOL000098	Tusizi	Quercetin	46.43335	0.27525
MOL000211	Huangqi	Mairin	55.37707	0.7761
MOL000239	Huangqi	Jaranol	50.82882	0.29148
MOL000296	Huangqi	Hederagenin	36.91391	0.75072
MOL000033	Huangqi	(3S,8S,9S,10R,13R,14S,17R)-10,13-dimethyl-17-[(2R,5S)-5-propan-2-yl]octan-2-yl]-2,3,4,7,8,9,11,12,14,15,16,17-dodecahydro-1H-cyclopenta[a]phenanthren-3-ol	36.22847	0.78288
MOL000354	Huangqi	Isorhamnetin	49.60438	0.306
MOL000371	Huangqi	3,9-di-O-methylnissolin	53.74153	0.47573
MOL000374	Huangqi	5'-hydroxyiso-muronulatol-2',5'-di-O-glucoside	41.71767	0.69251
MOL000378	Huangqi	7-O-methylisomucronulatol	74.68614	0.29792
MOL000379	Huangqi	9,10-dimethoxypterocarpan-3-O-β-D-glucoside	36.73669	0.9243
MOL000380	Huangqi	(6aR,11aR)-9,10-dimethoxy-6a,11a-dihydro-6H-benzofurano[3,2-c] chromen-3-ol	64.25545	0.42486
MOL000387	Huangqi	Bifendate	31.09782	0.66553
MOL000392	Huangqi	Formononetin	69.67388	0.21202
MOL000398	Huangqi	Isoflavanone	109.9867	0.29572
MOL000417	Huangqi	Calycosin	47.75183	0.24278
MOL000422	Huangqi	Kaempferol	41.88225	0.24066
MOL000433	Huangqi	FA	68.96044	0.7057
MOL000438	Huangqi	(3R)-3-(2-hydroxy-3,4-dimethoxyphenyl)chroman-7-ol	67.66748	0.26479
MOL000439	Huangqi	Isomucronulatol-7,2'-di-O-glucosiole	49.28106	0.62065
MOL000442	Huangqi	1,7-Dihydroxy-3,9-dimethoxy pterocarpene	39.04541	0.47943
MOL000098	Huangqi	Quercetin	46.43335	0.27525
MOL001006	Dangshen	Poriferasta-7,22E-dien-3beta-ol	42.97937	0.75555
MOL002140	Dangshen	Perlolyrine	65.94775	0.2747
MOL002879	Dangshen	Diop	43.59333	0.39247
MOL003036	Dangshen	ZINC03978781	43.82985	0.75647
MOL000449	Dangshen	Stigmasterol	43.82985	0.75665
MOL003896	Dangshen	7-Methoxy-2-methyl isoflavone	42.56474	0.19946
MOL004355	Dangshen	Spinasterol	42.97937	0.75534
MOL004492	Dangshen	Chrysanthemaxanthin	38.72398	0.58352
MOL005321	Dangshen	Frutinone A	65.90373	0.34184
MOL000006	Dangshen	Luteolin	36.16263	0.24552
MOL006554	Dangshen	Taraxerol	38.40254	0.76677

MOL006774	Dangshen	stigmast-7-enol	37.42312	0.75133
MOL007059	Dangshen	3-beta-Hydroxymethyllenetanshiquinone	32.16103	0.40894
MOL007514	Dangshen	Methyl icoso-11,14-dienoate	39.66706	0.22908
MOL008391	Dangshen	5alpha-Stigmastan-3,6-dione	33.1154	0.79021
MOL008393	Dangshen	7-(beta-Xylosyl) cephalomannine_qt	38.32746	0.28646
MOL008397	Dangshen	Daturilin	50.36513	0.76801
MOL008400	Dangshen	Glycitein	50.47891	0.23826
MOL008406	Dangshen	Spinoside A	39.96686	0.40288
MOL008407	Dangshen	(8S,9S,10R,13R,14S,17R)-17-[(E,2R,5S)-5-ethyl-6-methylhept-3-en-2-yl]-10,13-dimethyl-1,2,4,7,8,9,11,12,14,15,16,17-dodecahydrocyclopenta[a]phenanthren-3-one	45.40462	0.76174
MOL008411	Dangshen	11-Hydroxyrankinidine	40.00276	0.66203
MOL000020	Baishu	12-senecioid-2E,8E,10E-atractylentriol	62.39647	0.22294
MOL000021	Baishu	14-acetyl-12-senecioid-2E,8E,10E-atractylentriol	60.31287	0.30534
MOL000022	Baishu	14-acetyl-12-senecioid-2E,8Z,10E-atractylentriol	63.37092	0.29956
MOL000028	Baishu	α -Amyrin	39.51209	0.7629
MOL000033	Baishu	(3S,8S,9S,10R,13R,14S,17R)-10,13-dimethyl-17-[(2R,5S)-5-propan-2-yloctan-2-yl]-2,3,4,7,8,9,11,12,14,15,16,17-dodecahydro-1H-cyclopenta[a]phenanthren-3-ol	36.22847	0.78288
MOL000049	Baishu	3 β -acetoxyatractylone	54.06672	0.21906
MOL000072	Baishu	8 β -ethoxy atractylenolide III	35.95092	0.21079
MOL000273	Fuling	(2R)-2-[(3S,5R,10S,13R,14R,16R,17R)-3,16-dihydroxy-4,4,10,13,14-pentamethyl-2,3,5,6,12,15,16,17-octahydro-1H-cyclopenta[a]phenanthren-17-yl]-6-methylhept-5-enoic acid	30.93214	0.81281
MOL000275	Fuling	Trametenolic acid	38.7115	0.80199
MOL000276	Fuling	7,9(11)-dehydropachymic acid	35.10589	0.81091
MOL000279	Fuling	Cerevisterol	37.96383	0.77061
MOL000280	Fuling	(2R)-2-[(3S,5R,10S,13R,14R,16R,17R)-3,16-dihydroxy-4,4,10,13,14-pentamethyl-2,3,5,6,12,15,16,17-octahydro-1H-cyclopenta[a]phenanthren-17-yl]-5-isopropyl-hex-5-enoic acid	31.07206	0.81528
MOL000282	Fuling	ergosta-7,22E-dien-3beta-ol	43.50709	0.71939
MOL000283	Fuling	Ergosterol peroxide	40.36268	0.81255
MOL000285	Fuling	(2R)-2-[(5R,10S,13R,14R,16R,17R)-16-hydroxy-3-keto-4,4,10,13,14-pentamethyl-1,2,5,6,12,15,16,17-octahydrocyclopenta[a]phenanthren-17-yl]-5-isopropyl-hex-5-enoic acid	38.25516	0.82014
MOL000287	Fuling	3beta-Hydroxy-24-methylene-8-lanostene-21-oic acid	38.69991	0.8095
MOL000289	Fuling	Pachymic acid	33.62792	0.81076
MOL000290	Fuling	Poricoic acid A	30.60695	0.76152
MOL000291	Fuling	Poricoic acid B	30.5246	0.7463
MOL000292	Fuling	Poricoic acid C	38.15136	0.74643
MOL000296	Fuling	Hederagenin	36.91391	0.75072
MOL000300	Fuling	Dehydroeburicoic acid	44.1723	0.83458
MOL000359	Sangjisheng	Sitosterol	36.91391	0.7512

MOL000098	Sangjisheng	Quercetin	46.43335	0.27525
MOL003152	Xudian	Gentisin	64.06193	0.21335
MOL000358	Xudian	Beta-sitosterol	36.91391	0.75123
MOL000359	Xudian	Sitosterol	36.91391	0.7512
MOL009312	Xudian	(E,E)-3,5-Di-O-caffeoylquinic acid	48.14487	0.68394
MOL009317	Xudian	Cauloside A Qt	43.31716	0.81035
MOL008188	Xudian	Japonine	44.10725	0.24567
MOL009322	Xudian	Sylvestroside III	48.01755	0.52713
MOL009323	Xudian	Sylvestroside III Qt	56.46769	0.42632
MOL002058	Duzhong	40957-99-1	57.20447	0.61872
MOL000211	Duzhong	Mairin	55.37707	0.7761
MOL000358	Duzhong	Beta-sitosterol	36.91391	0.75123
MOL000422	Duzhong	Kaempferol	41.88225	0.24066
MOL004367	Duzhong	Olivil	62.2286	0.40642
MOL000443	Duzhong	Erythraline	49.17677	0.55031
MOL005922	Duzhong	Acanthoside B	43.35308	0.76689
MOL006709	Duzhong	AIDS214634	92.42724	0.54906
MOL007059	Duzhong	3-beta-Hydroxymethyllenetanishi quinone	32.16103	0.40894
MOL000073	Duzhong	Ent-Epicatchin	48.95984	0.24162
MOL007563	Duzhong	Yangambin	57.52545	0.80801
MOL009007	Duzhong	Eucommin A	30.51336	0.84815
MOL009009	Duzhong	(+)-medioresinol	87.18866	0.61875
MOL009015	Duzhong	(-)-Tabernemontanine	58.66918	0.60719
MOL009027	Duzhong	Cyclopamine	55.42172	0.82136
MOL009029	Duzhong	Dehydrodiconiferyl alcohol 4, gamma'-di-O-beta-D-glucopyranoside Qt	51.44226	0.39505
MOL009030	Duzhong	Dehydrodieugenol	30.10302	0.23906
MOL009031	Duzhong	Cinchonan-9-al, 6'-methoxy-, (9R)-	68.21502	0.40098
MOL009038	Duzhong	GBGB	45.57745	0.82668
MOL009042	Duzhong	Helenalin	77.01051	0.19049
MOL009047	Duzhong	(+)-Eudesmin	33.28664	0.62037
MOL009053	Duzhong	4-[(2S,3R)-5-[(E)-3-hydroxyprop-1-enyl]-7-methoxy-3-methylol-2,3-dihydrobenzofuran-2-yl]-2-methoxy-phenol	50.75514	0.3948
MOL009055	Duzhong	Hirsutin Qt	49.81498	0.37152
MOL009057	Duzhong	Liriodendrin Qt	53.13736	0.79961
MOL000098	Duzhong	Quercetin	46.43335	0.27525
MOL002773	Duzhong	Beta-carotene	37.18433	0.58358
MOL008240	Duzhong	(E)-3-[4-[(1R,2R)-2-hydroxy-2-(4-hydroxy-3-methoxy-phenyl)-1-methylol-ethoxy]-3-methoxy-phenyl]acrolein	56.31706	0.36095
MOL011604	Duzhong	Syringetin	36.82222	0.37414
MOL001559	Shanyao	Piperlonguminine	30.71143	0.1802
MOL001736	Shanyao	(-)-taxifolin	60.50622	0.27342
MOL000310	Shanyao	Denudatin B	61.47238	0.37838
MOL000322	Shanyao	Kadsurenone	54.72301	0.37829
MOL005429	Shanyao	hancinol	64.01327	0.37314
MOL005430	Shanyao	hancinone C	59.04593	0.38965
MOL005435	Shanyao	24-Methylcholest-5-enyl-3beta-O-glucopyranoside Qt	37.57682	0.71653
MOL005438	Shanyao	Campesterol	37.57682	0.71488
MOL005440	Shanyao	Isofucosterol	43.7764	0.7576
MOL000449	Shanyao	Stigmasterol	43.82985	0.75665
MOL005458	Shanyao	Dioscoreside C Qt	36.38229	0.87051
MOL000546	Shanyao	Diosgenin	80.87792	0.80979

MOL005461	Shanyao	Doradexanthin	38.15575	0.53662
MOL005463	Shanyao	Methylcimicifugoside qt	31.69349	0.23655
MOL005465	Shanyao	AIDS180907	45.32836	0.77301
MOL000953	Shanyao	CLR	37.8739	0.67677
MOL001484	Gancao	Inermine	75.18306	0.53754
MOL001792	Gancao	DFV	32.76272	0.18316
MOL000211	Gancao	Mairin	55.37707	0.7761
MOL002311	Gancao	Glycyrol	90.77578	0.66819
MOL000239	Gancao	Jaranol	50.82882	0.29148
MOL002565	Gancao	Medicarpin	49.21982	0.3351
MOL000354	Gancao	Isorhamnetin	49.60438	0.306
MOL000359	Gancao	Sitosterol	36.91391	0.7512
MOL003656	Gancao	Lupiwighteone	51.63569	0.36739
MOL003896	Gancao	7-Methoxy-2-methyl isoflavone	42.56474	0.19946
MOL000392	Gancao	Formononetin	69.67388	0.21202
MOL000417	Gancao	Calycosin	47.75183	0.24278
MOL000422	Gancao	Kaempferol	41.88225	0.24066
MOL004328	Gancao	Naringenin	59.2939	0.21128
MOL004805	Gancao	(2S)-2-[4-hydroxy-3-(3-methylbut-2-enyl)phenyl]-8,8-dimethyl-2,3-dihydropyrano[2,3-f]chromen-4-one	31.78703	0.72403
MOL004806	Gancao	Euchrenone	30.28726	0.57386
MOL004808	Gancao	Glyasperin B	65.22439	0.43851
MOL004810	Gancao	Glyasperin F	75.8368	0.53514
MOL004811	Gancao	Glyasperin C	45.56381	0.39947
MOL004814	Gancao	Isotrifoliol	31.94479	0.42422
MOL004815	Gancao	(E)-1-(2,4-dihydroxyphenyl)-3-(2,2-dimethylchromen-6-yl) prop-2-en-1-one	39.61686	0.35077
MOL004820	Gancao	kanzonols W	50.48008	0.51704
MOL004824	Gancao	(2S)-6-(2,4-dihydroxyphenyl)-2-(2-hydroxypropan-2-yl)-4-methoxy-2,3-dihydrofuro [3,2-g] chromen-7-one	60.25041	0.63433
MOL004827	Gancao	Semilicoisoflavone B	48.77755	0.54732
MOL004828	Gancao	Glepidotin A	44.72187	0.34685
MOL004829	Gancao	Glepidotin B	64.46292	0.34485
MOL004833	Gancao	Phaseolinisoflavan	32.00811	0.44538
MOL004835	Gancao	Glypallichalcone	61.59706	0.18993
MOL004838	Gancao	8-(6-hydroxy-2-benzofuranyl)-2,2-dimethyl-5-chromenol	58.43728	0.38106
MOL004841	Gancao	Licochalcone B	76.75735	0.1935
MOL004848	Gancao	Licochalcone G	49.25496	0.32325
MOL004849	Gancao	3-(2,4-dihydroxyphenyl)-8-(1,1-dimethylprop-2-enyl)-7-hydroxy-5-methoxy-coumarin	59.62247	0.42894
MOL004855	Gancao	Licoricone	63.57846	0.4712
MOL004856	Gancao	Gancaonin A	51.07519	0.40378
MOL004857	Gancao	Gancaonin B	48.7944	0.44924
MOL004860	Gancao	Licorice glycoside E	32.88743	0.27218
MOL004863	Gancao	3-(3,4-dihydroxyphenyl)-5,7-dihydroxy-8-(3-methylbut-2-enyl) chromone	66.37125	0.41392
MOL004864	Gancao	5,7-dihydroxy-3-(4-methoxyphenyl)-8-(3-methylbut-2-enyl) chromone	30.48878	0.41002
MOL004866	Gancao	2-(3,4-dihydroxyphenyl)-5,7-dihydroxy-6-(3-methylbut-2-enyl) chromone	44.15196	0.41482
MOL004879	Gancao	Glycyrin	52.60657	0.47466
MOL004882	Gancao	Licocoumarone	33.21085	0.3568

MOL004883	Gancao	Licoisoflavone	41.61022	0.41646
MOL004884	Gancao	Licoisoflavone B	38.92871	0.54714
MOL004885	Gancao	Licoisoflavanone	52.46625	0.54488
MOL004891	Gancao	Shinpterocarpin	80.29528	0.72746
MOL004898	Gancao	(E)-3-[3,4-dihydroxy-5-(3-methylbut-2-enyl)phenyl]-1-(2,4-dihydroxyphenyl)prop-2-en-1-one	46.26792	0.3062
MOL004903	Gancao	Liquiritin	65.69011	0.73893
MOL004904	Gancao	Licopyranocoumarin	80.36001	0.6535
MOL004905	Gancao	3,22-Dihydroxy-11-oxo-delta(12)-oleanene-27-alpha-methoxycarbonyl-29-oic acid	34.31942	0.54718
MOL004907	Gancao	Glyzaglabrin	61.06889	0.35347
MOL004908	Gancao	Glabridin	53.24514	0.46967
MOL004910	Gancao	Glabranin	52.89566	0.31208
MOL004911	Gancao	Glabrene	46.26686	0.43902
MOL004912	Gancao	Glabrone	52.51217	0.49645
MOL004913	Gancao	1,3-dihydroxy-9-methoxy-6-benzofurano[3,2-c] chromenone	48.14154	0.42831
MOL004914	Gancao	1,3-dihydroxy-8,9-dimethoxy-6-benzofurano[3,2-c] chromenone	62.90135	0.52759
MOL004915	Gancao	Eurycarpin A	43.27728	0.37429
MOL004917	Gancao	Glycyroside	37.25032	0.79156
MOL004924	Gancao	(-)-Medicocarpin	40.99397	0.95059
MOL004935	Gancao	Sigmoidin-B	34.88109	0.41455
MOL004941	Gancao	(2R)-7-hydroxy-2-(4-hydroxyphenyl) chroman-4-one	71.12299	0.18303
MOL004945	Gancao	(2S)-7-hydroxy-2-(4-hydroxyphenyl)-8-(3-methylbut-2-enyl) chroman-4-one	36.56537	0.32291
MOL004948	Gancao	Isoglycyrol	44.69923	0.83845
MOL004949	Gancao	Isolicoflavonol	45.16999	0.41859
MOL004957	Gancao	HMO	38.36542	0.21067
MOL004959	Gancao	1-Methoxyphaseollidin	69.98098	0.63739
MOL004961	Gancao	Quercetin der.	46.44939	0.3343
MOL004966	Gancao	3'-Hydroxy-4'-O-Methylglabridin	43.71495	0.57406
MOL000497	Gancao	Licochalcone a	40.78965	0.28517
MOL004974	Gancao	3'-Methoxyglabridin	46.16151	0.57393
MOL004978	Gancao	2-[(3R)-8,8-dimethyl-3,4-dihydro-2H-pyrano[6,5-f]chromen-3-yl]-5-methoxyphenol	36.21429	0.52122
MOL004980	Gancao	Inflacoumarin A	39.7091	0.32613
MOL004985	Gancao	Icos-5-enoic acid	30.70294	0.19725
MOL004988	Gancao	Kanzonol F	32.46833	0.89364
MOL004989	Gancao	6-prenylated eriodictyol	39.22383	0.41259
MOL004990	Gancao	7,2',4'-trihydroxy 5-methoxy-3 arylcoumarin	83.71437	0.27136
MOL004991	Gancao	7-Acetoxy-2-methylisoflavone	38.92333	0.26217
MOL004993	Gancao	8-prenylated eriodictyol	53.79476	0.40383
MOL004996	Gancao	Gadelaidic acid	30.70294	0.19725
MOL000500	Gancao	Vestitol	74.65519	0.20935
MOL0005000	Gancao	Gancaonin G	60.43521	0.39404
MOL0005001	Gancao	Gancaonin H	50.10372	0.78416
MOL0005003	Gancao	Licoagrocarpin	58.8139	0.58498
MOL0005007	Gancao	Glyasperins M	72.67081	0.59274
MOL0005008	Gancao	Glycyrrhiza Flavonol A	41.27528	0.59512
MOL0005012	Gancao	Licoagroisoflavone	57.28224	0.48679

MOL005013	Gancao	18 α -hydroxyglycyrrhetic acid	41.16139	0.7091
MOL005016	Gancao	Odoratin	49.94822	0.30487
MOL005017	Gancao	Phaseol	78.76622	0.57867
MOL005018	Gancao	Xambioona	54.84916	0.87419
MOL005020	Gancao	Dehydroglyasperins C	53.82326	0.37006
MOL000098	Gancao	Quercetin	46.43335	0.27525

Abbreviation, Traditional Chinese Medicine Systems Pharmacology (TCMSP) Database; Oral bioavailability, OB; Drug-likeness, DL.